

QUANTIFICATION IN SPECT: MYTH OR REALITY? A MULTI-CENTRIC STUDY

Sébastien Hapdey, Marine Soret, Ludovic Ferrer,
Pierre Malick Koulibaly, Jérôme Henriques, Isabelle Gardin,
Jacques Darcourt and Irène Buvat

Abstract— *Reliable quantification from Single Photon Emission Computed Tomography (SPECT) images could facilitate patient classification and follow-up. The purpose of this study was to assess the current performance of French nuclear medicine departments (NMD) and research centers (RC) in estimating parameters from SPECT images. A Tc99m SPECT brain study of the dopaminergic system was simulated using the Monte Carlo code SimSET. Projections corresponding to different energy windows, attenuation maps, anatomical images, characteristics of the detector response function, and parameters of the simulated acquisitions were made available on a Web site. The quantification task was to estimate four binding potential (BP) values measured on the left and right putamen and caudate nuclei. Four NMD and two RC participated in the study. Although they were equipped with recent workstations, NMD had limited access to sophisticated quantification tools, unlike RC, which could correct for scatter, attenuation, detector response function and even partial volume effect. Reported BP varied by factors greater than 3, due in part to differences in the corrections applied. Even for similar corrections, BP could differ by more than 50% between centres. Sophisticated processing performed by the RC yielded less biased and more reproducible BP estimates than processing available to NMD.*

In conclusion, this study suggests that large efforts are still required to make sophisticated processing tools available on commercial workstations equipping NMD, without which meta-analysis of values collected at different centers is impossible.

I. INTRODUCTION

Reliable estimation of tracer uptake or uptake ratios from Single Photon Emission Computed Tomography (SPECT) images could facilitate patient classification and patient follow-up. To that end, biases affecting SPECT images have been widely studied and corrections have been proposed, with encouraging results suggesting that accurate quantification is feasible (e.g., [1]). The purpose of this study was to assess the current performance of French nuclear medicine departments and research centers in estimating parameters from SPECT images. Correlated objectives were: 1) to study the inter-department variability in processing and results, and 2) to list the processing tools available in these departments for performing tasks frequently required for deriving quantitative parameters from SPECT images.

II. MATERIAL AND METHODS

A. Data

To circumvent the problem of “reference values” (i.e., knowing the “true values” to be estimated), datasets obtained with realistic Monte Carlo simulations were considered. A Tc-99m SPECT brain study of the dopaminergic neurotransmission system was simulated using SimSET [2]. Various activity levels were set on the putamen, cerebellum, caudate nuclei, cortex and rest of the brain (Table 1).

Table 1: Relative activity simulated in the different brain structures.

| Structure | Bgd | Cortex | Putamen | Caudate | Cerebellum |
|----------------|-----|--------|---------|---------|------------|
| Activity level | 1 | 2 | 5 | 4 | 2.2 |

The simulated data were obtained as follows: we simulated a high statistics acquisition, of approximately 3 billions photons in 128 projections over 360°. The projections were then blurred using a Gaussian filter with a FWHM ~ 4 mm, to mimic the intrinsic response of the camera crystal and associated electronics. The resulting noise-free projections were scaled in order to achieve a realistic count rate. Finally, Poisson noise was added to these “noise-free” projections, to get the noisy projections. The resulting data were made available on a Web site in raw format (flat file without any header) and in Interfile format. The provided data consisted in:

Manuscript received October 19, 2004. This work was supported by the French GDR STIC-Santé.

Sébastien Hapdey is with the department of nuclear medicine, Centre Henri Becquerel, Rouen, France, the Laboratoire Quant.I.F., Faculté de Médecine, Rouen, France and INSERM U494, Paris, France (e-mail: sebastien.hapdey@rouen.fnclec.fr, telephone: 33.2.08.24.78).

Marine Soret was with INSERM U494, Paris, France. She is now with the Hôpital Inter Armée, Val de Grâce, Paris, France (e-mail: soret@imed.jussieu.fr).

Ludovic Ferrer is with the Centre Gauducheau, Nantes, France and with INSERM U601, Nantes, France (e-mail: l-ferrer@nantes.fnclec.fr).

Pierre Malick Koulibaly and Jacques Darcourt are with the department of nuclear medicine, Centre Lacassagne, Nice, France, (e-mail: koulibal@unice.fr and jacques.darcourt@unice.fr) and with the department of biophysics, Faculté de Médecine, Nice, France.

Jérôme Henriques is with department of biophysics, Faculté de Médecine, Nice, France (e-mail: Jerome.henriques@unice.fr).

Isabelle Gardin is with the Centre Henri Becquerel, Rouen, France and Laboratoire Quant.I.F., Faculté de Médecine, Rouen, France (e-mail: isabelle.gardin@rouen.fnclec.fr).

Irène Buvat is with INSERM U494, 75013 Paris, France (e-mail: buvat@imed.jussieu.fr).

- 128 projections 128x128 with a pixel size of 2.2 mm, acquired in the 20% spectral window (from 126 to 154 keV).
- 128 projections 128x128 with a pixel size of 2.2 mm acquired in 16 spectral windows of equal width (4.75 keV) between 102 and 178 keV. This image series was intended for the users willing to perform scatter correction.
- The attenuation map (fig. 1) consisting of 120 slices 256 x 256 with a pixel size of 1.1 mm and a slice thickness of 1.4 mm, was used for the Monte-Carlo simulation with values expressed in cm^{-1} at 140 keV. The image dimensions were intentionally different from those of the projections. The images were also not perfectly aligned with the emission data (shifts of 4.3, 3.8 and 1.5 pixels in the transaxial (X and Y) and axial (Z) directions respectively, and rotations of 0.1 radians around the axial direction). This map was intended to be used for attenuation correction, after spatial registration with the emission data.
- An anatomical map (fig. 1) consisting of 120 slices 256 x 256 with a pixel size of 1.1 mm and a slice thickness of 1.4 mm, in which the different brain structures (cerebellum, cortex, insula, caudate nuclei, putamen, and rest of the brain) were labelled.

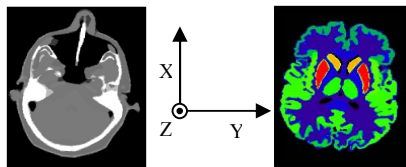


Fig. 1. Attenuation and anatomical maps used for the Monte-Carlo simulation. These maps were intentionally misaligned with the emission data (not shown here).

This map was aligned with the attenuation map. It was intended for the users willing to perform a partial volume effect correction, as the contours of the putamen and caudate nuclei were perfectly delineated in the anatomical images. In addition, the parameters of the SPECT acquisition that was simulated were listed: 128 projections acquired on a circular orbit (15 cm radius of rotation), with a LEHR collimator (hole radius of 1 mm, collimator thickness of 3.5 cm, septal thickness of 0.2 mm).

The relationship describing the variation of the spatial resolution FWHM (in mm) of the detector as a function of the object to collimator surface distance d (in mm) was also given as:

$$\text{FWHM}(d) = 0.02266 d + 5.445.$$

B. Data analysis

The quantification task to be performed was to estimate 4 binding potential (BP) values (2 for the left and right putamen and 2 for the left and right caudate nuclei), where BP was defined as:

$$BP = \frac{(A_{\text{structure}} - A_{\text{whitematter}})}{A_{\text{whitematter}}}$$

The simulated BP were 4 for the left and right putamen and 3 for the left and right caudate nuclei. As the simulated data mimicked real data, they should ideally be corrected for scatter, attenuation (using the attenuation map after it has been spatially registered with the emission data), detector response function and partial volume effect (PVE - using the anatomical images).

Table 2: Processing protocols used in the different NMD and RC and resulting BP values.

| | NMD1 | | NMD2 | | NMD3 | | NMD4 | | | | RC1 | | RC2 | |
|--------------------|---------------------|--------|--------------------------|--|---------------------|--------|---------------------|------|----------|------|------------------------------|--|------------------------------|---------|
| Data import | eNTEGRA/Vision | | Mirage | | Hermes | | Odyssey | | | | Sequin | | Sequin | |
| Display | eNTEGRA | | Mirage | | Hermes | | Odyssey | | | | Pixies | | Xdispm | |
| Scatter | n/a | | n/a | | n/a | | n/a | | Jaszczak | | Factor analysis (Pixies) | | TEW (Sequin) | |
| Image registration | n/a | | Automatic Rigid (Mirage) | | n/a | | n/a | | | | Manual rigid (Sequin) | | Automatic Rigid (Pixies) | |
| Detector response | n/a | | n/a | | n/a | | n/a | | | | FDP [§] | | FDP [§] | |
| Reconstruction | OSEM | FBP | OSEM | | HOSEM | | FBP | | | | OSEM | | OSEM | |
| Attenuation | n/a | Chang* | n/a | | n/a | Chang* | n/a | Ch* | n/a | Ch* | OSEM with μ map (Sequin) | | OSEM with μ map (Sequin) | |
| PVE correction | n/a | | n/a | | n/a | | n/a | | | | n/a | | n/a | Rousset |
| VOI drawing | Manual [°] | | Max in structure | | Manual [°] | | Manual [°] | | | | Manual [°] | | Anatomical [#] | |
| Left putamen BP | 1.14 | 1.06 | 1.53 | | 1.52 | 1.19 | 0.98 | 1.18 | 1.08 | 1.31 | 2.95 | | 1.26 | 3.26 |
| Right putamen BP | 1.21 | 1.11 | 1.36 | | 1.52 | 1.26 | 0.88 | 1.05 | 0.99 | 1.19 | 3.53 | | 1.11 | 2.88 |
| Left caudate BP | 0.93 | 0.86 | 1.53 | | 1.24 | 0.92 | 0.75 | 0.91 | 0.83 | 1.03 | 1.89 | | 0.69 | 1.56 |
| Right caudate BP | 0.96 | 0.91 | 1.18 | | 1.13 | 0.90 | 0.68 | 0.82 | 0.77 | 0.93 | 2.23 | | 0.71 | 1.81 |
| Processing | #1 | #2 | #3 | | #4 | #5 | #6 | #7 | #8 | #9 | #10 | | #11 | #12 |

[§] Correction using the Frequency Distance Principle

* Chang attenuation correction assuming uniform attenuation

[°] VOI manually drawn inside the structure of interest (putamen or caudate nucleus) to reduce partial volume effect

[#] VOI derived from the image of the anatomical compartment, matching the contours of the putamen and caudate nuclei.

Four nuclear medicine departments (NMD1 to NMD4) and 2 research centers (RC1 and RC2) participated in the study. Among the 4 NMD, NMD1 was equipped with Vision and eNTEGRA workstations (GE Medical System), NMD2 with a Mirage workstation (Segami), NMD3 with a Hermes workstation (Nuclear Diagnostics) and NMD4 with an Odyssey workstation (Philips). RC1 and RC2 were equipped with Sequin software (Système de QUantification en Imagerie Nucléaire), an image processing platform based on the Khoros environment and dedicated to SPECT and PET data. They were also equipped with Pixies software, which was used for scatter correction (RC1) or for image registration (RC2) (Apteryx, France; <http://www.apteryx.fr/pixies>).

Table 2 demonstrates that although they were equipped with recent workstations dedicated to clinical practice, NMD had limited access to sophisticated processing protocols, such as scatter and attenuation correction, image registration or partial volume correction. Only simple correction schemes were available. For scatter correction, the only method available was the subtraction of projections recorded in 2 different energy windows [3] (NMD4). For attenuation correction, only uniform attenuation correction using the Chang method (all NMD except NMD2) could be performed. None of the clinical workstations could successfully import the attenuation map associated with the data to be processed for non-uniform attenuation correction, because of the format of the provided data (raw or Interfile). This shortcoming could be avoided in the future by considering real phantom data instead of simulated data. None of the NMD could correct for depth-dependent detector response or partial volume effect.

III. RESULTS AND DISCUSSION

A. Processing protocols

Table 1 summarizes the processing performed by the NMD and RC, together with the resulting BP values.

Research centers had access to more sophisticated tools for performing the corrections needed when aiming at quantification. The two centers were able to correct for scatter, non-uniform attenuation using the provided attenuation map, and detector response function using the linear relationship between the FWHM and the source-to-collimator surface distance. Partial volume effect could be explicitly corrected for only at RC2 [1]. At RC1, VOIs manually drawn well inside the anatomical contours of the putamen and caudate nuclei were used to reduce the biases introduced by partial volume effect.

B. Binding potential values

Table 2 shows a great variability of the estimated BP values, which were, for instance, between 0.88 (#6) and 3.53 (#10) for the right putamen (true value was 4) and between 0.68 (#6) and 2.23 (#10) for the right caudate nuclei (true value was 3). Obviously, part of this variability was due to the different

corrections applied to the data. However, even for processing protocols including corrections for the same effects, results still differ substantially (fig. 2). For instance, without any correction and considering similar VOI measurements (NMD1 (#1), NMD3 (#4) and NMD4 (#6)), right putamen BP varied between 0.88 and 1.52, and right caudate nucleus BP varied between 0.68 and 1.13.

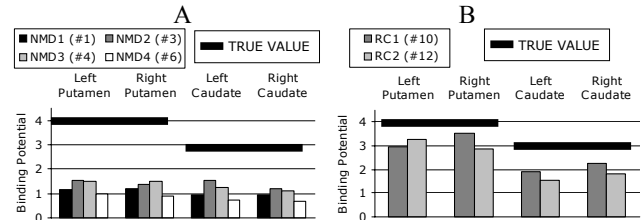


Fig. 1. BP estimates without any correction in NMD (A) or considering corrections for all effects in RC (B).

When performing corrections for all effects, errors in BP estimates were largely reduced. For instance, without any correction, the percent error (± 1 standard deviation) averaged over all NMD (processing #1, #3, #4, #6) in right putamen BP estimate was $-68\% \pm 7\%$, while for the most sophisticated processing protocols (processing #10, #12), the average percent error was $-20\% \pm 11\%$ (fig. 2)

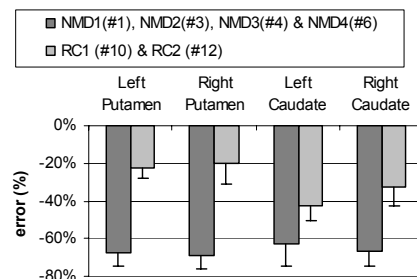


Fig. 2. Averaged error and associated standard deviation in the BP estimates considering uncorrected data (NMD1 (#1), NMD2 (#3), NMD3 (#4) & NMD4 (#6)) or the most sophisticated correction schemes (RC1(#10) & RC2 (#12)).

Also, for NMD4, which tested 4 processing protocols, the protocols including scatter and attenuation corrections performed the best (Table 2). Finally, RC1 and RC2 results suggest that although variability between estimated BP remains when supposedly quantitative processing are used, it is less than variability affecting measurements performed on uncorrected data: mean BP variability for NMDs was $24.3\% \pm 4.5$ vs $12.4\% \pm 3.6$ for RCs, where BP variability (%) was defined as $[\text{standard deviation}(\text{BP}) / \text{mean}(\text{BP})]$. This decrease in variability can be partly explained by the increase of BP values brought by the correction.

IV. CONCLUSION

This work gave evidence of the large variability of parameter estimates performed at various institutions, making it impossible any meta-analysis of values collected at different institutions. Part of the variability was obviously due to

differences in corrections applied to the data, the most sophisticated corrections being not available to NMD. Large efforts are still required to make sophisticated processing tools available on commercial workstations equipping NMD as such tools definitely improve the accuracy of parameter estimates and reduce their variability.

V. REFERENCES

- [1] M. Soret, P.M. Koulibaly, J. Darcourt, S. Hapdey and I. Buvat, "Quantitative accuracy of dopaminergic neurotransmission imaging using 123I SPECT", *J. Nucl. Med.*, vol. 44, pp. 1184-1193, 2003.
- [2] R.L. Harrison, S.D. Vannoy, D.R. Haynor, S.B. Gillispie, M.S. Kaplan and T.K. Lewellen, "Preliminary experience with the photon history generator module of a public-domain simulation system for emission tomography", *Conf record of the IEEE Nuclear Science Symposium*, vol. 2, pp. 1154-1158, 1993.
- [3] R.J. Jaszcak, C.E. Floyd and R.E. Coleman, "Scatter compensation techniques for SPECT", *IEEE Transactions on Nuclear Science*, vol. NS-32, pp. 786-793, 1985.